

Soft Matter

Accepted Manuscript



This is an *Accepted Manuscript*, which has been through the Royal Society of Chemistry peer review process and has been accepted for publication.

Accepted Manuscripts are published online shortly after acceptance, before technical editing, formatting and proof reading. Using this free service, authors can make their results available to the community, in citable form, before we publish the edited article. We will replace this *Accepted Manuscript* with the edited and formatted *Advance Article* as soon as it is available.

You can find more information about *Accepted Manuscripts* in the [Information for Authors](#).

Please note that technical editing may introduce minor changes to the text and/or graphics, which may alter content. The journal's standard [Terms & Conditions](#) and the [Ethical guidelines](#) still apply. In no event shall the Royal Society of Chemistry be held responsible for any errors or omissions in this *Accepted Manuscript* or any consequences arising from the use of any information it contains.



Journal Name

ARTICLE

Dynamically controlled deposition of colloidal nanoparticles suspension in evaporating drops using laser radiation

V. D. Ta,^{a,†} R. M. Carter^a, E. Esenturk^b, C. Connaughton^{b,c}, T. J. Wasley^d, J. Li^d, R. W. Kay^d, Jonathan Stringer^{e,f}, P. J. Smith^e and J. D. Shephard^a

Received 00th January 20xx,
Accepted 00th January 20xx

DOI: 10.1039/x0xx00000x

www.rsc.org/

The dynamic control of the distribution of polystyrene suspended nanoparticles in evaporating droplets is investigated using a 2.9 μm high power laser. Under laser radiation a droplet is locally heated and fluid flows are induced that overcome the capillary flow, thus a reversal of the coffee-stain effect is observed. Suspension particles are accumulated in a localised area, one order of magnitude smaller than the original droplet size. By scanning the laser beam over the droplet particles can be deposited in an arbitrary pattern. This finding raises the possibility for direct laser writing of suspended particles through a liquid layer. Furthermore, a highly uniform coating is possible by manipulating the laser beam diameter and exposure time. The effect is expected to be universally applicable to aqueous solutions independent on solutes (either particles or molecules) and deposited substrates.

Introduction

Self-assembly processes are important phenomena because they have a significant impact on the development of biological systems, creation of ensembles of nanostructures and photonic devices.¹⁻⁷ An example of such a process observed in everyday life would be a coffee drop leaving a ring-like stain once completely evaporated. This process is referred to as the coffee-ring or coffee-stain effect and is frequently observed in most evaporating droplets of micro-/nano-particle suspensions.⁸⁻¹¹ This effect has recently attracted a great deal of interest due to the profound influence in many scientific and technical areas.^{11,12}

The coffee-stain effect can be useful for several applications such as assembly of line structures¹³ and nanochromatography.¹⁴ However, due to non-uniform deposition it is undesirable for applications requiring uniform coating, such as high resolution ink-jet printing¹⁵,¹⁶ and biotechnology.^{17,18} To overcome this effect, several

techniques have been proposed by manipulating capillary flows, changing particle shape and modifying the surface wettability of the substrate.^{11,19-25} However, the ability to dynamically control the distribution of the suspended particles during evaporation of droplets has rarely been studied.

It has been shown that infrared light increases surface temperatures of aqueous fluids, and therefore, affects the capillary flow of aqueous droplets.²⁶ This result opens up the opportunity to modify the coffee-stain effect by external radiation. In addition, as lasers have excellent coherence and strong intensities, it is more appropriate compared with a broadband light source for tuning the coffee-stain effect. Indeed, simulations have demonstrated that laser-induced motion in droplets of nanoparticle suspensions greatly influences the final distribution of the particles.²⁷ However, to our knowledge, experimental investigation of this effect has not been studied.

In this work, an infrared laser operating at 2.9 μm is used to study the ability to dynamically control the deposition of nanoparticles in evaporating drops.

Theoretical background

Transport of particles within an evaporating droplet is a complex process where a number of physical effects are involved. However, as it was reviewed in Larson Survey,²⁸ dimensional analysis reveals the mechanisms that have the largest influence in determining the final deposition patterns. Under the conditions of our experimental setup, mass, momentum and heat transfer effects are more dominant while other effects are of secondary importance. Therefore the governing mathematical equations, assuming cylindrical symmetry, can be set up as follows:

^a Institute of Photonics and Quantum Sciences, Heriot-Watt University, Edinburgh, EH14 4AS, UK

^b Warwick Mathematics Institute, Zeeman Building, University of Warwick, Coventry CV4 7AL, UK

^c Centre for Complexity Science, Zeeman Building, University of Warwick, Coventry CV4 7AL, UK

^d Additive Manufacturing Research Group, Loughborough University, Leicestershire, LE11 3TU, UK

^e Laboratory of Applied Inkjet Printing, Department of Mechanical Engineering, University of Sheffield, Sheffield, S1 4BJ, UK

^f Department of Mechanical Engineering, The University of Auckland, Auckland 1142, New Zealand

[†] Corresponding Author, Email address: d.ta@hw.ac.uk

Electronic Supplementary Information (ESI) available: Figures S1-S3 show three dimensional profile of formation patterns. Figure S4 demonstrates optical image of distribution of dye molecules on a glass substrate without and with laser radiation. Movies S1-S4 demonstrate the coffee-stain effect, reverse of the coffee-stain effect and uniform deposition. See DOI: 10.1039/x0xx00000x

$$\partial c(x, t) / \partial t = D \Delta c \quad (1)$$

where c is the vapor concentration, D is the diffusivity $x = (r, z)$ denotes a spatial point r and z being the radial and vertical coordinates.

Coupled to the mass-balance equation we have the energy balance equation in the form of the heat equation given as

$$\partial T(x, t) / \partial t = K \Delta T + q(x, t) \quad (2)$$

where K is the thermal conductivity and q is the heat input-rate per unit volume due to laser radiation.

These equations are solved subject to the appropriate boundary conditions. To determine the evaporation dynamics one has to solve these coupled sets of equations and is work that will be done explicitly in a forthcoming paper.

Experimental section

Material

Polystyrene (PS) suspension (~0.3% solids) was used in all experiments. It was obtained by diluting commercial 2% solids PS monodisperse aqueous suspension (microspheres, particle size of 0.5 μm , standard deviation < 0.05 μm , Sigma-Aldrich) with deionized water. To obtain a uniform dispersion, the solution was put in an ultrasonic bath for ~10 minutes. The substrate used for droplet deposition was a 1 mm-thick stainless steel sheet (304S15, RS components).

Optical setup

The laser beam from a continuous wavelength Sheamann DRV-002 compact high power laser with a wavelength of ~2.9 μm was guided and focused (focal plane is at the substrate surface) normally to the substrate. The irradiated droplet was monitored by a Unibrain 1394 camera at angle of ~40° to the normal of the substrate. Furthermore, the laser spot was captured and analyzed using an infrared camera (Electrophysics, PV320). All experiments were done at ambient conditions with temperature of ~22°C and relative humidity of 30-45 %.

Surface characterization

Three-dimensional (3D) profiles of the final distributions of the PS nanoparticles were obtained by an Alicona microscope (using z-stack measurement provided from IF-MeasureSuite Version 5.1). Prior to optical measurement, the samples were coated with a thin metallic layer (Chromium, ~0.8 μm) through RF sputtering. This is done to improve surface reflectivity and thus obtain improved signal from the microscope.

Results and discussion

Water has a strong absorption at 2.9 μm ,²⁹ which dictated the selection of the infrared laser used in this work. The irradiated laser energy is absorbed by the water drop and this radiation energy is

transferred to heat, which results in a temperature gradient and strong evaporating flux at the illuminated region. Fig. 1 shows the schematic of the optical setup where a droplet is heated by a focused beam normal to the surface. In addition, as the laser beam diameter gradually decreases from the focused lens to the droplet, the effect of laser diameter on the distribution of PS nanoparticles could be studied by simply translating the substrate vertically through the laser beam (z direction). The substrate could also be translated relative to the laser in the y direction.

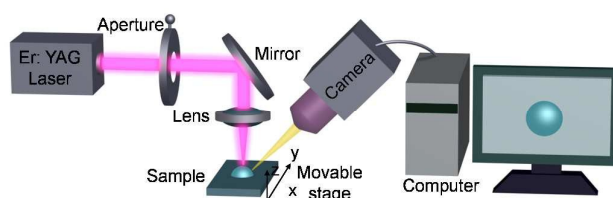


Fig. 1 Schematic of optical setup used for controlling and observing deposition of colloidal nanoparticles in evaporating droplets.

Figs. 2a and 2b present the final distribution of PS nanoparticles without external radiation and with laser irradiation, respectively. It can be seen that the patterns indicate a typical “coffee-stain” and a reverse of “coffee-stain”, respectively. For the first case, all material was deposited at the rim of the droplet. In contrast, for the second, nearly all particles were accumulated to a ~0.7 mm-diameter spot at the central region of the droplet. In order to get measure the particle distribution in the vertical (z) direction, a 3D surface morphology of these samples was measured out and the results are presented in Figs. S1 and S2 (Supplementary Information).

Figs. 2c and 2d plot the cross-section profiles of the patterns (extracted from the above 3D distribution). For the “coffee-ring” structure, there are two clear peaks in the edge representing high particle accumulation whereas in the middle there is essentially zero particle deposition (Fig. 2c). In contrast, for the reverse of “coffee-ring” pattern, the profile shows a high density of particles in the middle of the droplet with comparatively few particles at the edge (Fig. 2d). The pattern height of the laser-induced structure is ~120 μm , which is 4 times larger than ~30 μm of the ring. The result demonstrates that infrared laser beams can effectively attract suspension particles and accumulate them in an area that is much smaller than the original droplet size.

The mechanism of the coffee-stain effect has been well-studied.^{8,9} As shown in Fig. 2e, the contact line remains pinned during evaporation thus the contact angle decreases, which results in capillary flow from the droplet’s centre to its rim, and a corresponding ring-like structure is obtained (Supporting video 1).¹¹ Conversely, when the droplet is illuminated with a laser beam, it is locally heated at the irradiated region and the localized heating induces flow. This process overcomes the capillary flow and leads to the accumulation of particles towards the laser spot (supporting video 2).

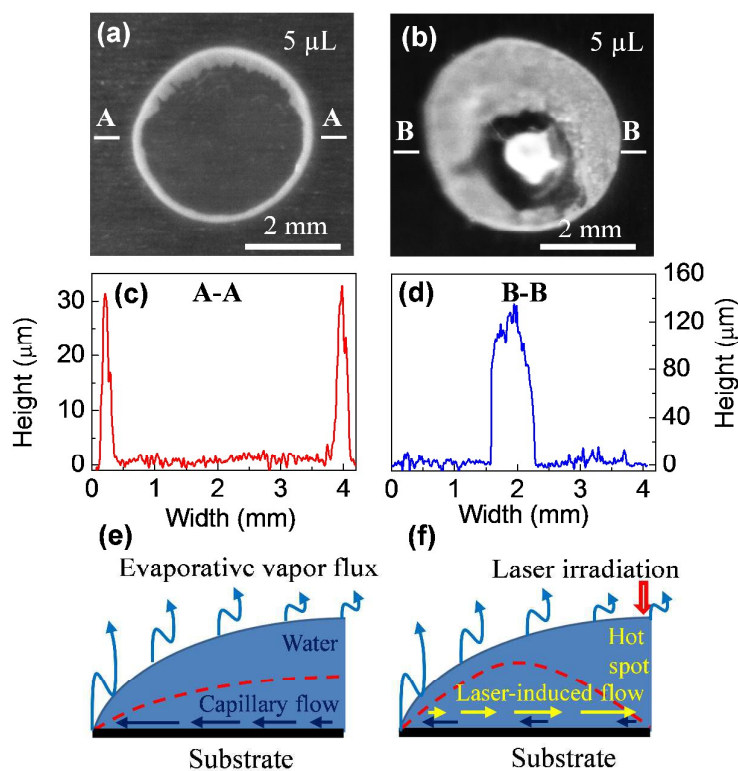


Fig. 2 (a), (b) Optical image of the final distributions of PS particles obtained under ambient conditions without and with laser irradiation, respectively. The sample was positioned at the focal plane and laser spot was ~ 0.43 mm in diameter. (c), (d) Cross-section profiles of the pattern shown in (a) and (b), respectively. (e), (f) Schematic diagram of the evaporation process for the two cases. The dashed line represents the droplet profile towards the end of evaporation.

It is suggested that the effect of laser radiation leads to two major flows: (i) the thermo-capillarity due to temperature gradient^{26, 27} and (ii) the replenishing of the large amount of water lost by intense radiation. Previous work has shown that the presence of recirculating Marangoni flows acts to reverse the coffee-stain effect.¹⁹ In the same work it was also stated that such flows do not tend to occur in water, with the experimentally determined flow being orders of magnitude lower than that determined by theory. The temperature gradient imposed by the incident laser, however, is orders of magnitude greater than that observed in ambient conditions, which may be sufficient to induce a Marangoni flow.

The intense radiation and subsequent heating will also lead to significantly greater evaporation at the center of the droplet compared to the edge; in direct opposition to the relative evaporative loss observed in ambient conditions.⁸ This effect can consequently lead to a reversal of flow due to evaporative loss of liquid and contribute to the accumulation of particles.

It is worth noting that other effects such as optical trapping and modification of the particles due to laser heating are negligible because of following reasons. Firstly, the laser energy is strongly absorbed by the water in the aqueous suspension at the droplet's surface. Indeed, at 2.9 microns the absorption of water is around

10^6 m⁻¹. This gives a penetration depth of only ~ 1 micron. Secondly, the PS particles constitute only a tiny fraction ($\sim 0.3\%$) of the solution. Their motion is predominantly determined by the flow of the liquid which is a common assumption in the literature. Finally, the low concentration one can safely assume that the PS particles and the liquid in the immediate neighbourhood have the same temperature at any time which will not cause any heat-driven local disturbance. Furthermore, the collective diffusion of charged PS particles driven by long-ranged interactions such as the electrostatic interaction³⁰ is also insignificant as the net interaction of the PS particles is believed to be short range.

As discussed above, the higher temperature at the point of heating causes a reversal of flow, which is primarily responsible for the accumulation of particles at droplet's centre. To support this idea, the evaporation time (measured from the time a droplet is deposited until the evaporation is complete) for drops with and without external radiation (represented as t_{fL} and t_f , respectively) was investigated. Fig. 3 shows that t_f is at least one order of magnitude longer than t_{fL} . For example, it takes ~ 60 min for a typical 6 μL-droplet to completely dry but only ~ 5 to 1.5 min when it is irradiated with a power density of 53 and 224 W/cm², respectively. The fast evaporation means large fluid loss at the point of heating, and therefore, fluid will flow from other parts of the droplet towards the laser spot to replenish.

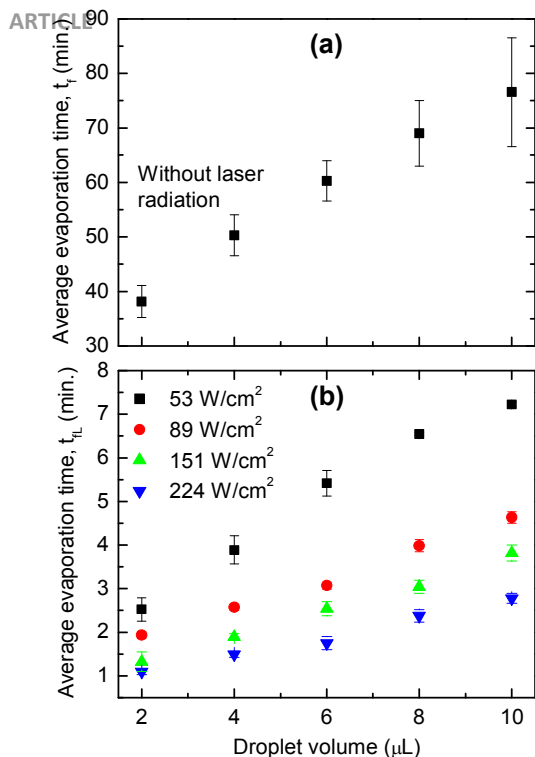


Fig. 3 Average evaporation time for droplets with various fluid volumes under ambient conditions. (a) Without laser irradiation. (b) With differing laser intensity. The sample was at the focal plane with laser spot of ~ 0.43 mm in diameter. The error bars are the standard deviation of the average of three individual measurements per point.

The effect of droplet volume on the final distribution of the particles was studied. Figs. 4a-4c presents the pattern for 3, 7, and 15 μL - droplets, respectively. It is clear that droplet size does not strongly influence the pattern formation as a reverse coffee-stain effect is observed for the three cases. However, the ring-like structure becomes more obvious (more particles go to the edge) with an increase of droplet size. For a larger droplet the evaporation time is longer hence the particles have more time to transfer from the droplet centre to the edge via capillary flow. As a result, more particles are deposited at the rim and thus make the contact line visible.

The ability to concentrate nanoparticles to selected areas (within a droplet) with arbitrary configurations has potential applications in biotechnology,¹⁸ assembly of colloidal nanomaterials,³¹ and disordered photonic devices such as random lasers.^{32, 33} Fig. 4d indicates a high particle density spot can be obtained toward the edge of the droplet. It is also possible to distribute particles in multiple locations within the confines of the droplet by sequentially illuminating more than one location during droplet evaporation. In Fig. 4e, the laser beam was irradiated at position 1 for $\sim 0.65t_{\text{ev}}$ (t_{ev} is the total evaporation time of a droplet when it is exposed to the laser) and moving to position 2 afterward where the laser was kept

motionless until the evaporation is complete. Interestingly, a line structure can be achieved by moving the droplet relative to the laser beam (Fig. 4f). It is expected that more complex structures can be fabricated using a galvanometer scan head or using a mask,³⁴ which raises the possibility for direct laser writing of suspended particles through a liquid layer.

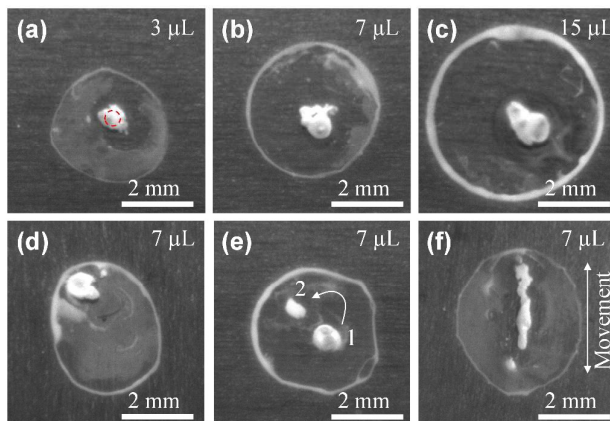


Fig. 4 Pattern formation for PS nanoparticles under laser irradiation with various conditions. (a)-(c) Laser spot was at the central region of the droplet. (d) Laser spot was located at the top left in the image of the droplet. (e) Laser spot was at position 1 and then moved to position 2. (f) The substrate was moved relative to the laser beam with a constant speed of ~ 0.12 mm/s. All droplets were irradiated with ~ 0.43 mm-diameter laser spot, represented as a dash circle in (a), and power density of $151 \text{ W}/\text{cm}^2$. Droplet volume is indicated in the top-right of each image.

A uniform coating is highly desirable for applications such as ink-jet printing.^{15, 16} Several approaches have been investigated for homogeneous deposition by controlling the shape of particles¹¹ or using surfactant and surface-adsorbed polymer.³⁵ Other alternative is controlling evaporative fluid flow. Modifying evaporation rate is possible to enhance the classical coffee-stain effect or produce a total flow inversion,³⁶ and uniform deposition is thus suggested to be possible by balancing the two opposing processes. The use of an imposed temperature gradient to control the flow of solute within a droplet has been previously demonstrated by varying the substrate temperature.¹⁶ Similar results to those presented herein were found, with suppression of coffee staining found to occur when the temperature in the centre of the droplet was higher than at the edge.

We demonstrate two methods that have the potential to achieve homogeneous deposition. The first approach is by increasing the ratio between the laser diameter and the droplet size (the laser power is unchanged). The second is through shortening the exposure time. However, both techniques have the same physical

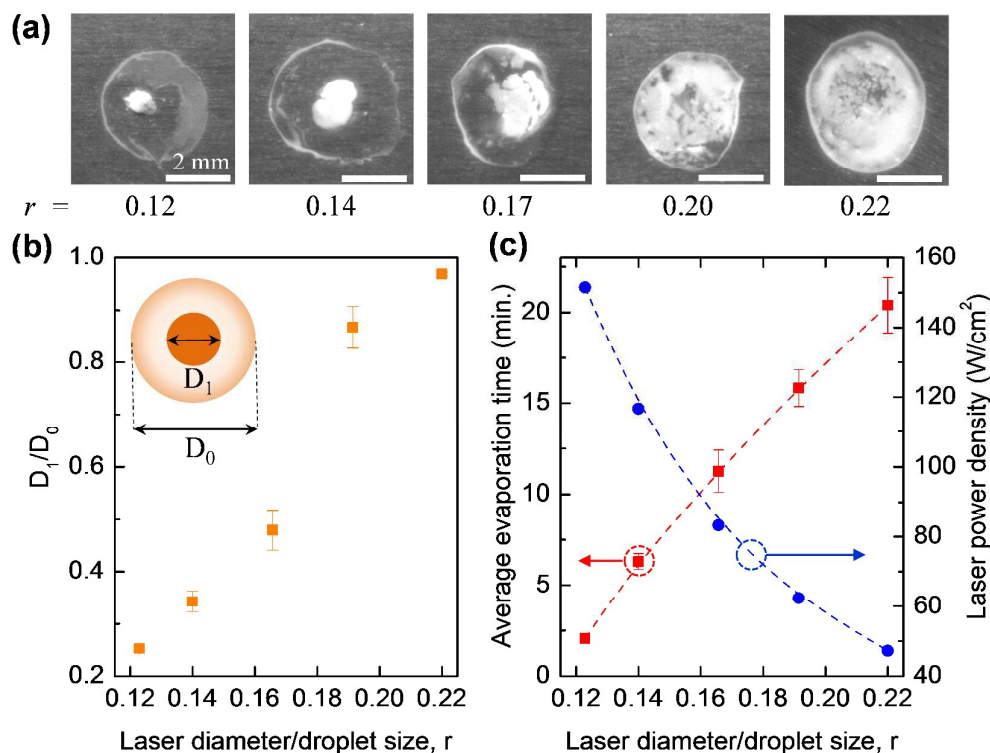


Fig. 5 (a) Pattern formation of PS nanoparticles with increase of laser spot characterized by the ratio (r) between laser beam diameter and initial droplet size (estimated to be ~ 3.5 mm). (b) Ratio between the spot with high particle density and the droplet size as a function of r . (c) Evaporation time and laser power density versus r . All droplets have the same volume of ~ 5 μL and the scale bars are 2 mm. The error bars are the standard deviation of the average of three individual measurements per point.

mechanism. It has been indicated (Fig. 2f) that when a droplet is illuminated at the central region by a laser beam, there will be primarily two opposing processes. The capillary flow drives particles from the centre of the droplet to the edge and the laser-induced flows force particles to go to the centre. Overall, if the capillary flow is dominant, the formed pattern will tend towards a coffee-stain-like appearance. Otherwise, the reverse of coffee-stain will be obtained. As a result, uniform deposition is only possible when the two processes are in equilibrium, which can be achieved by manipulating laser parameters.

In Fig. 5a, the pattern formed demonstrates a clear transition from the reverse of the coffee-stain to uniform coating by increasing the laser diameter. To get a quantitative evaluation, it is assumed that the droplet size and the spot at the droplet's centre (which has the highest particle density) are both circular with diameters of D_1 , D_0 , respectively (the inset of Fig. 5b). With this assumption, D_1/D_0 can be plotted as a function of r – the ratio between the laser diameter and the initial droplet size (estimated to be ~ 3.5 mm for ~ 5 μL droplets). From Fig. 5b, it can be seen that D_1/D_0 increases sharply with r . For $r = 0.12$, D_1/D_0 is only 0.25 but it shows a significant increase to 0.48 when r rises to 0.17. For r around or smaller than 0.17, particles are still accumulated in the central region of the

droplet. However, when r reaches 0.22, particles are distributed over a region that is over 90% of the droplet area (supporting video 3). The 3D profile of the formation pattern was measured and presented in Fig. S3 (Supplementary Information). The result indicates that a highly uniform distribution of PS particles was achieved.

The obtained results above can be explained by the change of laser power density. As shown in Fig. 5c, when the laser diameter increases, its power density decreases (as the power of the laser beam is fixed during the experiments) so that evaporation time increases correspondingly. As discussed earlier, for $r < 0.17$ the evaporation time is short (< 10 min), the laser-induced flows dominate over the capillary flow so the reverse of the coffee-stain effect is obtained. However, as the laser diameter becomes larger, and the laser power density decreases, the evaporation time increases. This gives time for the thermal energy from the radiation to dissipate into the bulk of the droplet and reduce the thermal gradient induced by the laser. This in turn reduces the flow of particles towards the laser spot and allows the conventional capillary flow to have greater influence on particle motion. It was found that the two competing flows became balanced when $r = 0.22$, thus a uniform coating was obtained.

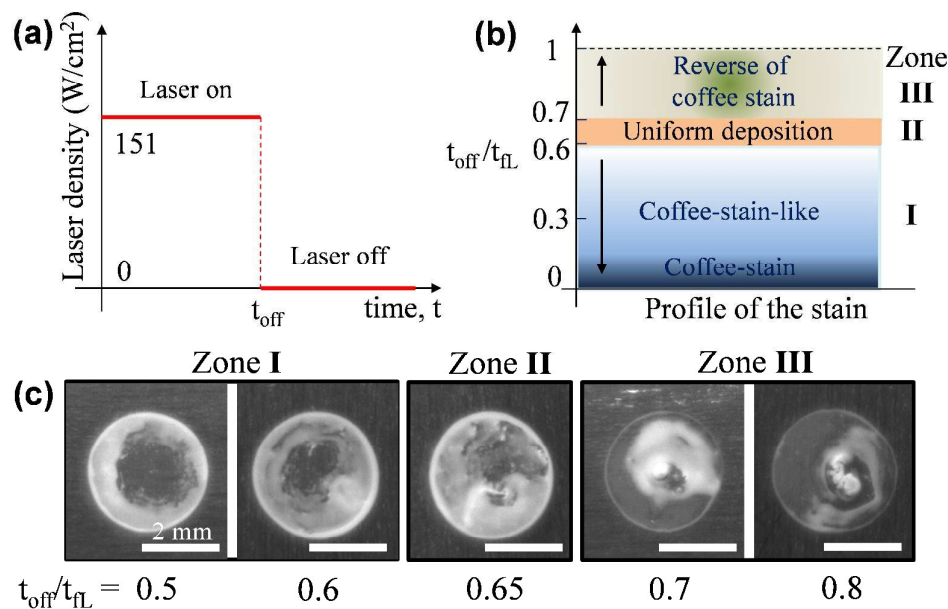


Fig. 6 (a) The schematic diagram shows the method for obtaining a uniform coating. The droplet is only illuminated for a certain time (t_{off}). After that, the laser is blocked and the droplet is leaved for drying spontaneously. (b) Characteristic of formation pattern as function of $t_{\text{off}}/t_{\text{FL}}$. (c) Optical images of final pattern versus $t_{\text{off}}/t_{\text{FL}}$. All scale bars are 2 mm and droplets have the same volume of $\sim 5 \mu\text{L}$.

The second approach to get a uniform deposition is by shortening the exposure time; the working principle is schematically demonstrated in Fig. 6a. Firstly, a droplet is irradiated by a laser beam for a certain time, the so-called t_{off} , which is normally less than the t_{FL} (discussed earlier in Fig. 3b). After that time the laser radiation is blocked and at that moment the evaporation is not complete. This process initially drives particles to the centre of the droplet while irradiated. The droplet was then left to dry without external heating. During this time, the capillary flow will spread particles, which were highly accumulated in the central region, to the whole droplet area. By varying the t_{off} , patterns with different properties are observed (Fig. 6b). Clearly, if $t_{\text{off}} = 0$, the droplet is not heated by the laser so a typical coffee-stain will be obtained. When $0 < t_{\text{off}}/t_{\text{FL}} < 0.6$ (referred as zone 1) the resulting pattern is a coffee-stain-like structure while $0.6 < t_{\text{off}}/t_{\text{FL}} \leq 1$ (zone 3) results in a reverse of coffee-stain. There is a narrow window where $t_{\text{off}}/t_{\text{FL}} \sim 0.65$ (zone II), an approximate uniform coating is obtained (supporting video 4). Fig. 6c shows formation patterns for $t_{\text{off}}/t_{\text{FL}} = 0.5-0.8$, where the transition from the coffee-stain-like structure to uniform coating and reverse of coffee-stain is clearly seen.

It is proposed that the laser induced-flows primarily affect the aqueous suspension. As a result, with a slight modification of laser parameters, similar results can be obtained for different solutes such as PS nanospheres with standard size of $0.1 \mu\text{m}$ and organic molecules. Fig. S4 (Supplementary Information) shows a reversal of the coffee-stain and uniform deposition for droplets containing Rhodamine B molecules and deposited on a glass substrate. As a

result, our approach should be universally applicable to a variety of research fields, with the proviso that the imposed temperature is not large enough to affect the eventual functionality of the formed pattern. An example of a potential application would be in biotechnology where a facile method for arbitrarily patterning tissues and biomarkers would be desirable.³⁷

Conclusions

The effect of laser diameter, laser power density and exposure time on fluid flows, evaporation time and resultant distribution of suspended nanoparticles in evaporating droplets has been demonstrated. Due to the localized heating, laser-induced flows drive particles to move and accumulate in any chosen area (within the droplet) with a selective pattern size. Deposited spots can be one order of magnitude smaller than the initial droplet size. This effect has potential applications for biotechnology and disordered photonic devices where high particle density and minimizing deposition space is highly important. Interestingly, by scanning the laser beam over the droplet, particles can be deposited in an arbitrary pattern, which opens an opportunity for direct laser writing through suspension liquids. Uniform coatings can also be achieved by manipulating laser diameter or exposure time, which has potential significance for applications requiring uniform coatings such as ink-jet printing.

Data availability

All relevant data present in this publication can be accessed at <http://dx.doi.org/10.17861/222eda1f-ba44-42e9-8e6e-ab7f9d1095f4>

Acknowledgements

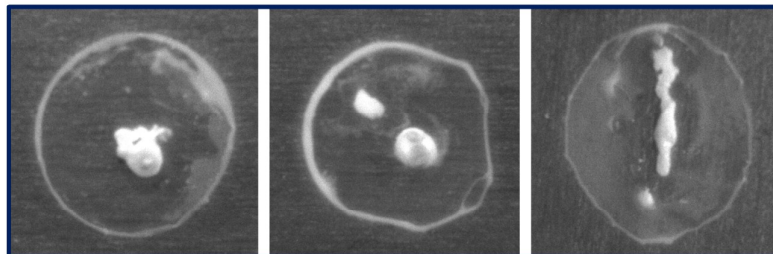
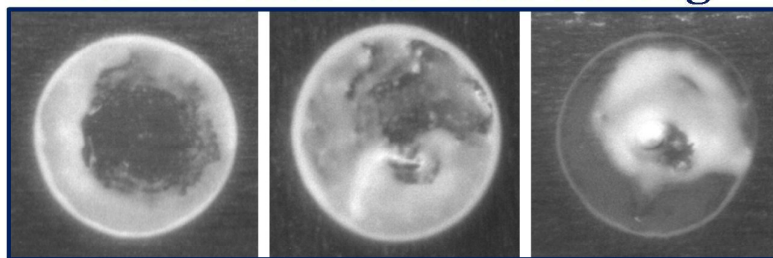
This work is funded by the UK Engineering and Physical Sciences Research Council under grants EP/L017431/1, EP/L017350/1, EP/L016907/1 and EP/L017415/1.

References

- G. M. Whitesides and B. Grzybowski, *Science*, 2002, **295**, 2418-2421.
- J. Xu, J. F. Xia, S. W. Hong, Z. Q. Lin, F. Qiu and Y. L. Yang, *Phys. Rev. Lett.*, 2006, **96**.
- E. Rabani, D. R. Reichman, P. L. Geissler and L. E. Brus, *Nature*, 2003, **426**, 271-274.
- M. Byun, R. L. Laskowski, M. He, F. Qiu, M. Jeffries-El and Z. Q. Lin, *Soft Matter*, 2009, **5**, 1583-1586.
- V. D. Ta, R. Chen and H. D. Sun, *Adv. Mater.*, 2012, **24**, OP60-OP64.
- J. F. Galisteo-López, M. Ibisate, R. Sapienza, L. S. Froufe-Pérez, Á. Blanco and C. López, *Adv. Mater.*, 2011, **23**, 30-69.
- V. D. Ta, R. Chen, D. M. Nguyen and H. D. Sun, *Appl. Phys. Lett.*, 2013, **102**, 031107.
- R. D. Deegan, O. Bakajin, T. F. Dupont, G. Huber, S. R. Nagel and T. A. Witten, *Nature*, 1997, **389**, 827-829.
- H. Hu and R. G. Larson, *J. Phys. Chem. B*, 2002, **106**, 1334-1344.
- T. P. Bigioni, X.-M. Lin, T. T. Nguyen, E. I. Corwin, T. A. Witten and H. M. Jaeger, *Nat. Mater.*, 2006, **5**, 265-270.
- P. J. Yunker, T. Still, M. A. Lohr and A. G. Yodh, *Nature*, 2011, **476**, 308-311.
- W. Han and Z. Q. Lin, *Angew. Chem.-Int. Edit.*, 2012, **51**, 1534-1546.
- S. Magdassi, M. Grouchko, D. Toker, A. Kamysny, I. Balberg and O. Millo, *Langmuir*, 2005, **21**, 10264-10267.
- T.-S. Wong, T.-H. Chen, X. Shen and C.-M. Ho, *Anal. Chem.*, 2011, **83**, 1871-1873.
- J. Park and J. Moon, *Langmuir*, 2006, **22**, 3506-3513.
- D. Soltman and V. Subramanian, *Langmuir*, 2008, **24**, 2224-2231.
- R. Blossey and A. Bosio, *Langmuir*, 2002, **18**, 2952-2954.
- V. Dugas, J. Broutin and E. Souteyrand, *Langmuir*, 2005, **21**, 9130-9136.
- H. Hu and R. G. Larson, *J. Phys. Chem. B*, 2006, **110**, 7090-7094.
- H. B. Eral, D. M. Augustine, M. H. G. Duits and F. Mugele, *Soft Matter*, 2011, **7**, 4954-4958.
- A. Crivoi and F. Duan, *J. Phys. Chem. B*, 2013, **117**, 5932-5938.
- Y.-F. Li, Y.-J. Sheng and H.-K. Tsao, *Langmuir*, 2013, **29**, 7802-7811.
- J. Mu, P. Lin and Q. Xia, *Appl. Phys. Lett.*, 2014, **104**, 261601.
- V. D. Ta, A. Dunn, T. J. Wasley, J. Li, R. W. Kay, J. Stringer, P. J. Smith, C. Connaughton and J. D. Shephard, *Appl. Surf. Sci.*, 2016, **365**, 153-159.
- D. Noguera-Marín, C. L. Moraila-Martínez, M. A. Cabrerizo-Vílchez and M. A. Rodríguez-Valverde, *Langmuir*, 2014, **30**, 7609-7614.
- A. K. Thokchom, A. Gupta, P. J. Jaijus and A. Singh, *Int. J. Heat Mass Transfer*, 2014, **68**, 67-77.
- M. Dietzel and D. Poulikakos, *Phys. Fluids*, 2005, **17**, 102106.
- R. G. Larson, *AIChE Journal*, 2014, **60**, 1538-1571.
- J. E. Bertie and Z. Lan, *Appl. Spectrosc.*, 1996, **50**, 1047-1057.
- A. Merlin, J. Angly, L. Daubersies, C. Madeira, S. Schöder, J. Leng and J.-B. Salmon, *Eur. Phys. J. E*, 2011, **34**, 58.
- Y. Gao, V. D. Ta, X. Zhao, Y. Wang, R. Chen, E. Mutlugun, K. E. Fong, S. T. Tan, C. Dang, X. W. Sun, H. Sun and H. V. Demir, *Nanoscale*, 2015, **7**, 6481-6486.
- D. S. Wiersma, *Nat. Phys.*, 2008, **4**, 359-367.
- Y. Wang, V. D. Ta, Y. Gao, T. C. He, R. Chen, E. Mutlugun, H. V. Demir and H. D. Sun, *Adv. Mater.*, 2014, **26**, 2954-2961.
- S. N. Varanakkottu, M. Anyfantakis, M. Morel, S. Rudiuk and D. Baigl, *Nano Lett.*, 2016, **16**, 644-650.
- H. Kim, F. Boulogne, E. Um, I. Jacobi, E. Button and H. A. Stone, *arXiv preprint arXiv:1602.07937*, 2016.
- A. Marin, R. Liepelt, M. Rossi and C. J. Kahler, *Soft Matter*, 2016, **12**, 1593-1600.
- S. V. Murphy and A. Atala, *Nat Biotech*, 2014, **32**, 773-785.

A table of contents entry:

Particle deposition in a homogeneous or arbitrary distribution can be obtained by direct exposure to an infrared laser beam

Laser-directed particle patterning**Laser-directed uniform coating**

Coffee-stain-like

Uniform coating

Reverse of coffee-stain-like

